Science Advances
AAAS

Supplementary Materials for

Electroluminescence of atoms in a graphene nanogap

Hyungsik Kim, Young Duck Kim, Tong Wu, Qingrui Cao, Irving P. Herman, James Hone, Jing Guo, Kenneth L. Shepard*

*Corresponding author. Email: shepard@ee.columbia.edu

Published 21 January 2022, *Sci. Adv.* **8**, eabj1742 (2022)
DOI: 10.1126/sciadv.abj1742

The PDF file includes:

Other Supplementary Material for this manuscript includes the following:

Supplementary Text

S1. Surface roughness and thickness of PECVD graphene

The surface roughness and thickness of PECVD graphene were measured by atomic force microscopy (AFM). Figure S2 shows the results of these AFM measurement. Surface roughness of PECVD graphene is 489 pm r.m.s. over a 20-μm-by-20-μm area (Fig. S2-A, B). Fig. S2-C, D shows the thickness of patterned PECVD graphene, which is approximately 10nm. Fig. S3 shows an TEM scanning image in the area of 2 μm × 2 μm (A) and 1 μm × 1 μm (B) of PECVD graphene.

S2. Thermal radiation

The Blackbody spectrum is given by Planck's Law:

$$I(\omega) \propto \frac{\omega^3}{\left[\exp\left(\frac{\hbar\omega}{k_B T}\right)-1\right]},$$

where I(ω) is the light intensity, ω is frequency, T is temperature, $\hbar$ is the reduced Plank's constant, and k_B is Boltzmann's constant. The spectrum at different blackbody temperatures is given in Fig. S5.

S3. Nanogap formation and endurance of I-V characteristics

A nanogap forms in the presence of a source-drain bias across the graphene channel layer. The resulting current-voltage characteristics at each stage of nanogap formation are shown in Fig. S6. Before and after nanogap formation, the peak current is reduced as shown in Fig. S7. There is some variation in green light emission with bias as shown in Fig. S8. This transition voltage shows some device geometry (Fig. S9) but is unaffected by back-gate biasing on the Si substrate as shown in Fig. S10. After nanogap formation, the transition behavior shows relatively stable I-V characteristics over many sweep cycles as shown in Fig. S11. It also shows endurance with time as shown in Fig. S12.

S4. hBN (hexagonal Boron Nitride) substrate effect

We use a poly-carbonate (PC) coated polydimethylsiloxane (PDMS) mounted on a glass slide to pick up and release hBN. PECVD graphene directly grown on SiO_2/Si substrate is placed on a vacuum hot plate stage under a microscope. The glass slide having PC-coated PDMS is placed on the PECVD graphene sample. When the polymer adheres to the overall surface of PECVD graphene, temperature of the hot plate ramps up to 150 °C by 4 °C/min for 30 min and then ramps down to 40 °C. Following this, the glass slide is slowly shifted away from the PECVD graphene sample along the z-axis of the micromanipulator in the vacuum hot plate. In this process, the glass slide picks up the PECVD graphene against the SiO_2/Si substrate. In order to pick up hBN on PECVD graphene, the glass slide attached to the PECVD graphene is slowly lowered until the polymer outside the PECVD graphene on the glass slide fully contacts the exfoliated hBN on the SiO_2/Si substrate. Similar to the original pick-up of the PECVD graphene, the temperature of the hot plate ramps up to 180 °C by 7.75 °C /min for 20 min. The glass slide is moved away from the hBN substrate as slowly as possible. The result is PECVD graphene/hBN/SiO_2/Si substrate with the polymer between the layers. In order to promote the adhesion of the PECVD graphene and hBN, the sample is baked on a hot plat at 200 °C for 10 min. Finally, the polymer is dissolved in chloroform for 12 hours.

After the PECVD graphene transfer process, we fabricate metal electrodes (Cr/Pd/Au, 2nm/30nm/50nm) on the sample. The metal deposition was conducted in e-beam evaporator, and we used a lift-off process and e-beam lithography (see Methods). The fabricated device, as shown in Fig. S13-A, was measured in vacuum environment (10^{-4} Torr). I-V characterization and EL measurement were conducted while monitoring light emission from the device.

S5. Exfoliated graphene light emission

An exfoliated graphene device having two electrodes was fabricated to measure light emission as shown in Fig. S14A. The material characteristics of the exfoliated graphene were detetmined by Raman spectroscopy in the area of channel as shown in Fig. S14B. The exfoliated graphene was transfered onto SiO_2 (~285nm)/Si (500 μm) substrate. After formation of electrodes on it, Raman spectroscopy has been measured to check intrinsic properties of graphene. The 3μm×3μm graphene area was patterned by dry etching using CHF_3 and O_2, while a lift-off process was used to define the electrodes. Lift-off method is used to pattern channel layer and electrodes. Poly(methyl methacrylate) (MicroChem PMMA A4 495 and A2 950) was coated in 2000 rpm and 1000 rpm for 1 minute on the sample. Following this, the sample was baked on hot plate at 180◦C for 2 minutes. For lithography, e-beam lithography was used (EBL, Nano Neam, NB4). To avoid shorting between contact and interconnect layers, islands of insulating hydrogen silsesquioxane (HSQ) were created, which were patterned by e-beam lithography. To develop the pattern, IPA solution mixed with MIBK as 3:1 stored under -5 ◦C in the fridge was used. Cr/Pd/Au of 1 nm/30 nm/50 nm and Cr/Au of 1 nm/50 nm were deposited as metal electrodes in an electron-beam evaporator. After this, lift-off was done in acetone for 1 hour. These lithography, deposition, and lift-off procedures were repeated for each layer. Fig. S14C shows green light emission from the PECVD graphene after nanogap formation.

S6. TEM measurement

The cross section of the measured device in Fig. S17 shows Cr/Au 5 nm/300 nm labeled as metal, SiO_2 ~285 nm, graphene 5 nm, graphene oxide ~20nm, and Si substrate 500 μm. Focused ion-beam (FIB), FEI Helios NanoLab 660, has been utilized to prepare cross-sectional samples for examination in the transmission electron microscope (TEM). In order to protect the graphene layers against the ion-beam damage during sample preparation, amorphous platinum (2-μm-thick) has been deposited on the device by electron and ion-beams, respectively. Scanning TEM (STEM) and high-resolution TEM (HRTEM) analyses have been performed using an FEI Talos F200X S-TEM at an accelerating voltage of 200 kV.

S7. XPS measurement

XPS (X-ray Photoemission Spectroscopy) measurement was conducted about pristine PECVD graphene, graphene nanogap light-emitting array, and oxidized PECVD graphene in a 1100 °C furnace as shown in Fig. S18. XPS analysis has been performed using an Phi 5500 XPS at an accelerating voltage of 15 kV and an power of 100W with an Mg X-ray source.

Table S1 shows deconvolved XPS data as shown in Fig. S18. sp2 and sp3 bonding is reduced in the nanogap array with graphene oxide and in the oxygen-annealed PECVD graphene. From Table S1, the graphene nanogap array has more oxygen-carbon bonding than pristine PECVD graphene. Specifically, the C-O-C bonding ratio increased up to 58.42% from 9.69% in pristine PECVD graphene. This increased amount mainly results from the graphene oxide.

S8. Unconventional behavior in electron transport

Fig. S20-A and S20-B show typical IV characteristics of N and S type NDR device, respectively. In Fig. S20-A, the dash lines mean band-to-band tunneling current, excess current, and diffusion current.

After nanogap creation, IV characteristics were measured as shown in Fig. S20-C, which have neither the N- or S-type characteristics. A forward sweep in V_{ds} bias shows a current drop at ~12V. As shown in Fig. S20-C, there is little to no excess current in the IV characteristic beyond the current drop.

S9. DFT calculation

We use the Virtual Nanolab Atomistix ToolKit. Density mesh cut-off is set as 100 Hartrees. K point sampling is 1 × 1 × 100. When plot the I-V curve, we sweep voltage bias from 0 to 3V with a 91 points grid and energy from -2 to 2 eV with 201 points. Bias can be calculated by the difference in Fermi level on the two side of the device structure. Zero energy is defined by the average of these two Fermi levels. When calculating the transmission, we sweep the energy from -3eV to 3eV with a 601 grid. Default parameters for the simulation are 2.09 Å between O and C, 3.70 Å between O and O, and 1.28 Å between C and C (Fig. S22).

S10. N-doped graphene light emission

We use nitrogen-doped graphene synthesized by CVD. Unlike CH_4 and H_2 used in conventional CVD graphene, a nitrogen-containing pyridine (C_5H_5N) was used as a liquid precursor. The test tube of CVD equipment was heated to 1000 °C for 40 min under the flow of hydrogen (H_2, 50 sccm) and Argon (Ar, 100 sccm) gases at ambient pressure. Following this, the argon supply was shut off and a copper foil was annealed for 20 min with hydrogen environment (H_2, 50 sccm flow). And then pyridine was vaporized at a pressure of 1.0×10^{-1} Torr. The nitrogen-doped graphene was deposited for 1 min.

S11. Quantum efficiency

External quantum efficiency (EQE) can be calculated from:

$EQE = \frac{2qN}{i} = \frac{2q}{i}\frac{1}{e_{N_k}}\sum_{i=1}^{2399}(N_i \cdot u_i)$,

where $q = 1.6 \times 10^{-19}$, $e_{N_k} = 4.98 \times 10^{-4}$, $i = current \times \frac{measured\ area}{emission\ area}$, N_i is a measured spectrum data from a photodetector, and u_i is a response data normalized to a 514.53-nm laser, which is powered as 1.3072×10^{-13}W. Measured EL data is converted to the number of photons based on the normalization. Because a nanogap is approximately one dimensional, the emission area is N□r^2, which N is the number of oxygen atoms and > 3×10^{18} at 300 K, and r is 3.7×10^{-11} m atomic radius. Assuming this results in an emission area of 1nm × 5μm, the EQE for green light emission is estimated to be 0.21%, but there is considerable uncertainty in this value.

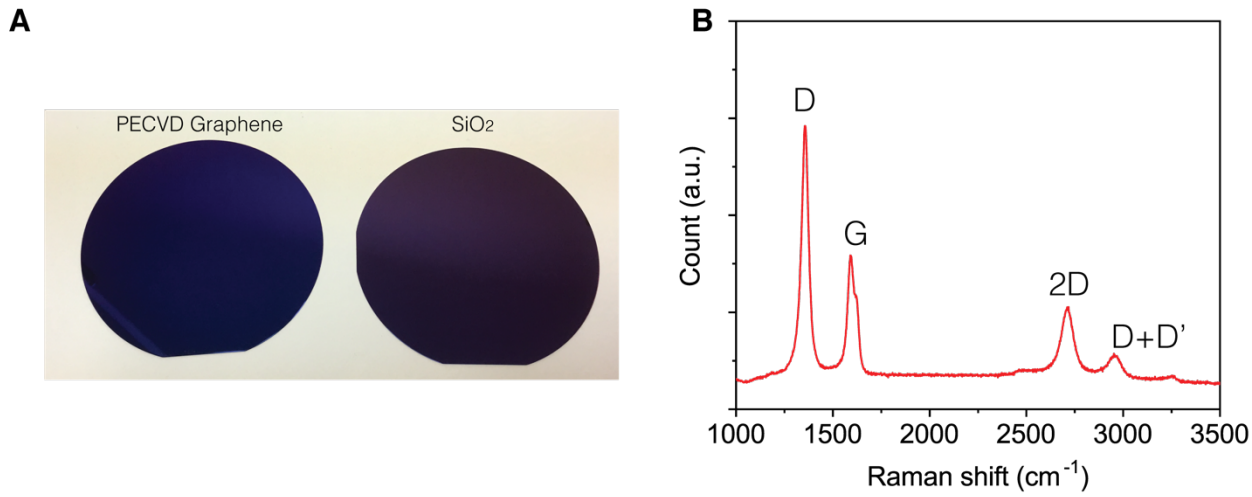

Fig. S1.
PECVD graphene wafers and Raman spectra. (A), Four-inch wafer scale growth of PECVD graphene and SiO_2. **(B)**, Raman spectra of PECVD graphene (red).

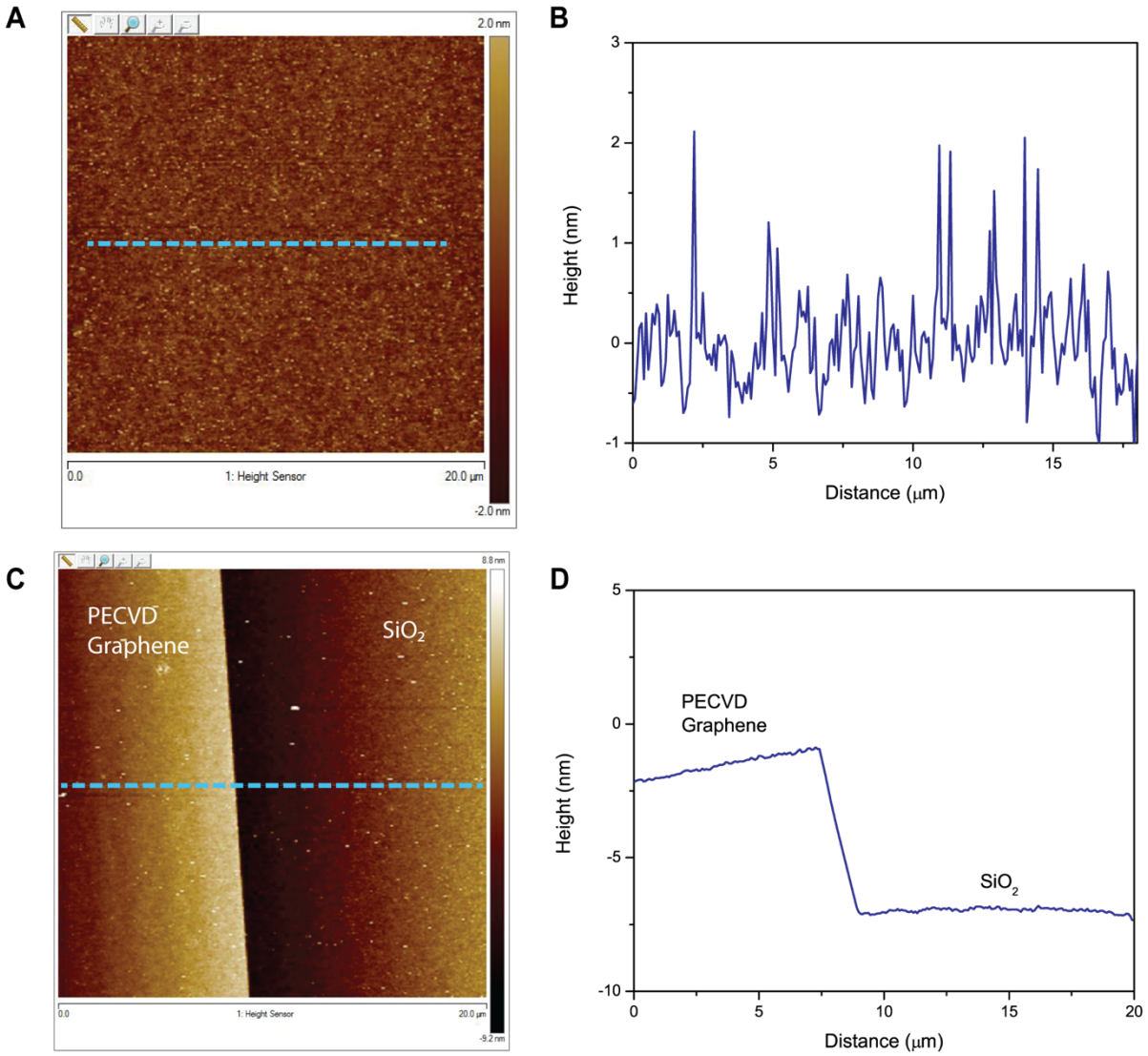

Fig. S2.

AFM measurement. A. An AFM scanning image in the area of 20 µm × 20 µm shows 489 pm r.m.s. **B.** Surface roughness in the cross section of **A**. **C.** An AFM scanning image of patterned PECVD graphene in the area of 20 µm × 20 µm (the left side: PECVD graphene, the right side: SiO_2). **D.** The step height of the patterned PECVD graphene.

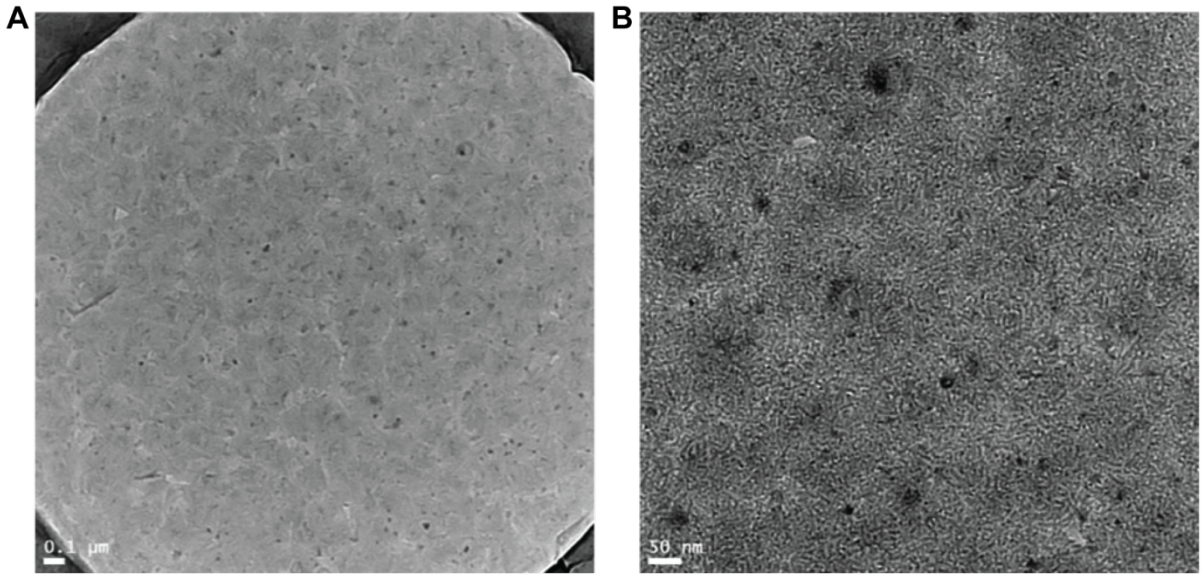

Fig. S3.

TEM measurement. An TEM scanning image in the area of 2 μm × 2 μm (A) and 1 μm × 1 μm (B) of PECVD graphene.

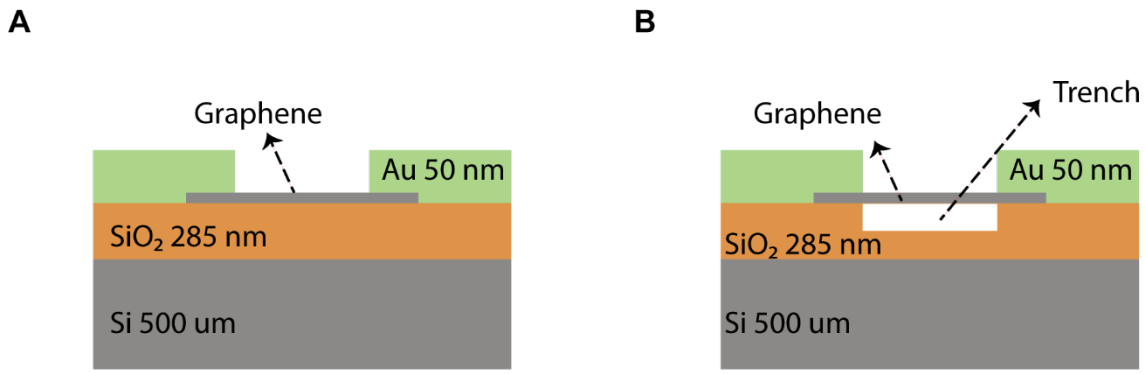

Fig. S4.
Device Structures. Suspended (A) and the non-suspended (B) structures.

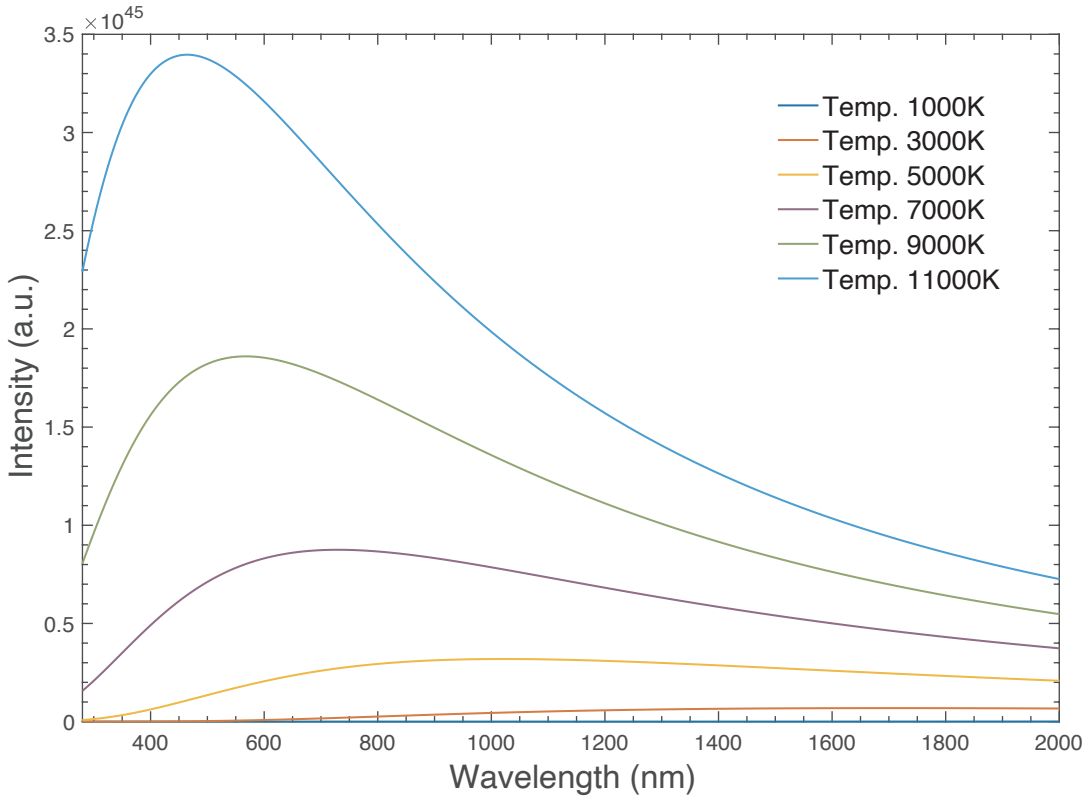

Fig. S5.
Black-body radiation along with temperature. Green light radiation requires 9000 K.

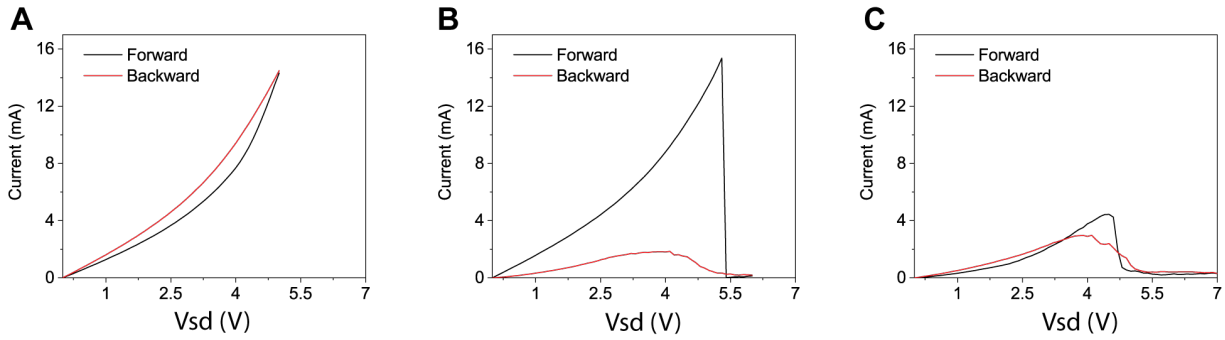

Fig. S6.

IV characterization at each stage for nanogap formation (W=7 µm, L=1 µm). A, IV characteristic up to 5 V sweeps in forward and backward directions before nanogap formation. **B,** IV characteristic up to 6 V sweeps in forward and backward directions at the moment of nanogap formation. The nanogap is formed at ~5.2 V when the current drops. **C,** After the nanogap formation, IV characteristic up to 7V sweeps in forward and backward directions.

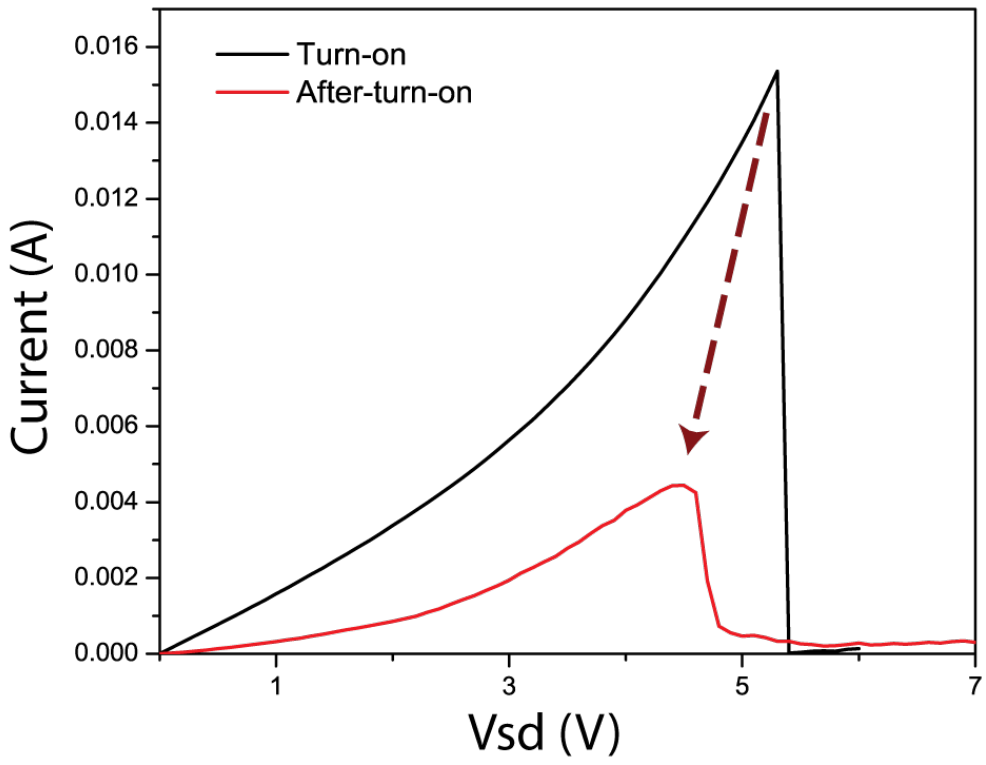

Fig. S7.

Current reduction after nanogap formation (W=7 µm, L=1 µm). Before and after nanogap formation, the peak current is reduced as shown in brown arrow and the voltage at the peak current is decreased by 0.8V.

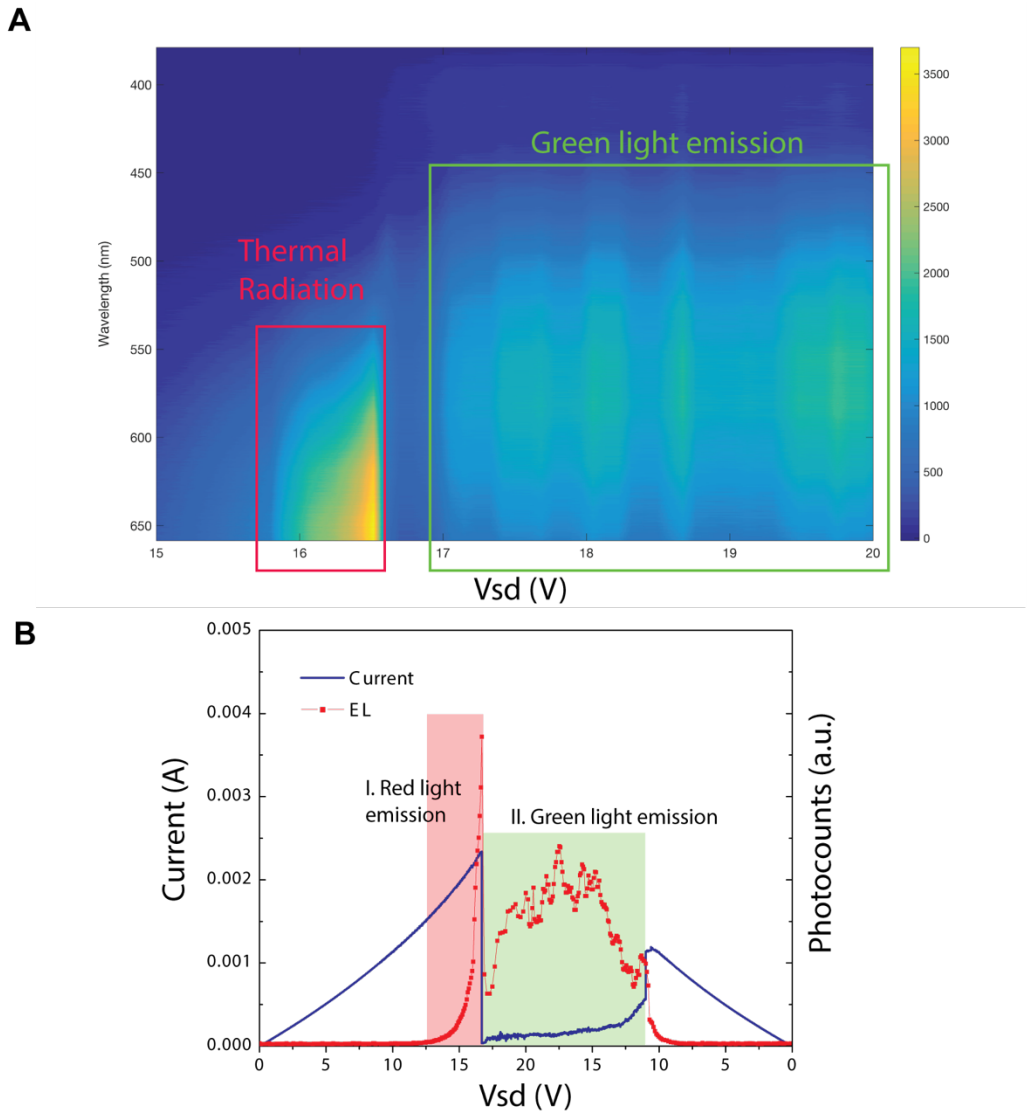

Fig. S8.

Electroluminescence (EL) measurement in W=L=5 µm. A, EL spectra in forward direction of bias. **B**, IV characteristic with peak EL photocounts from (A).

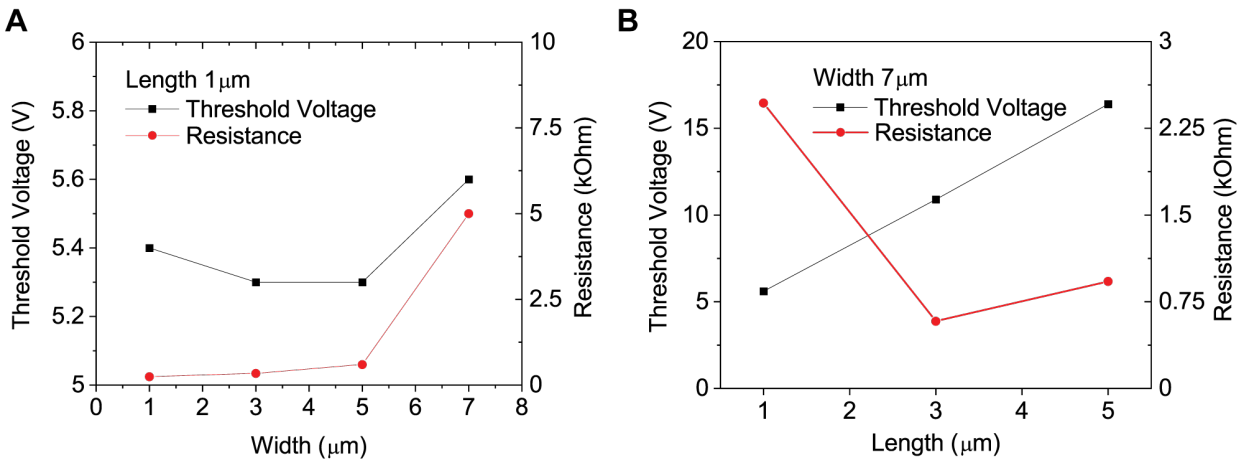

Fig. S9.

Threshold voltage and resistance for nanogap formation. Width (A) and length (B) variation change threshold voltage and resistance. Resistance is estimated by current at each threshold voltage.

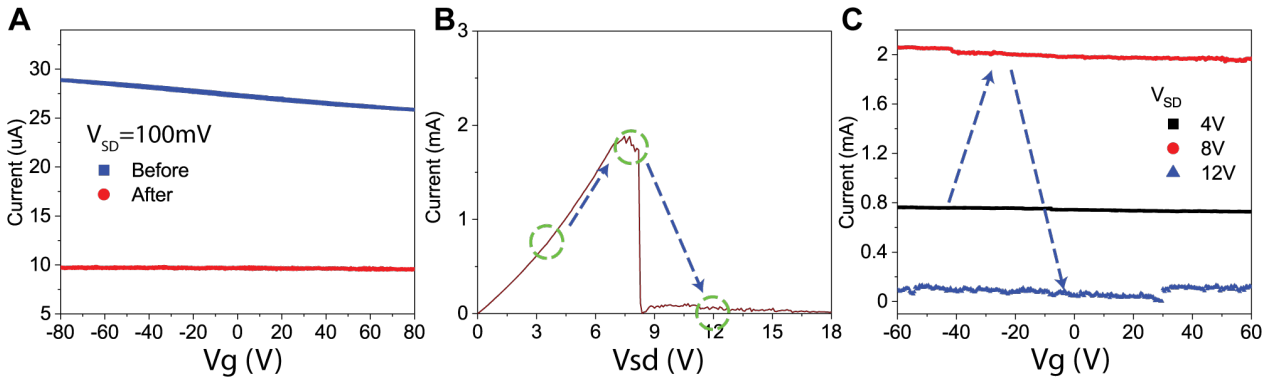

Fig. S10.

Back-gate bias effect in the nanogap channel for W=5 µm, L=5 µm. A, Back gate bias sweeps from -80 V to 80 V before and after nanogap formation. The weak gate voltage dependence prior to nanogap formation is consistent with unipolar hole transport. **B**, Conventional electron transport in the nanogap device. Green circles in 4, 8, 12 V are points for back gate bias test. **C**, Back gate bias effect at 4 V, 8 V, and 12 V, respectively.

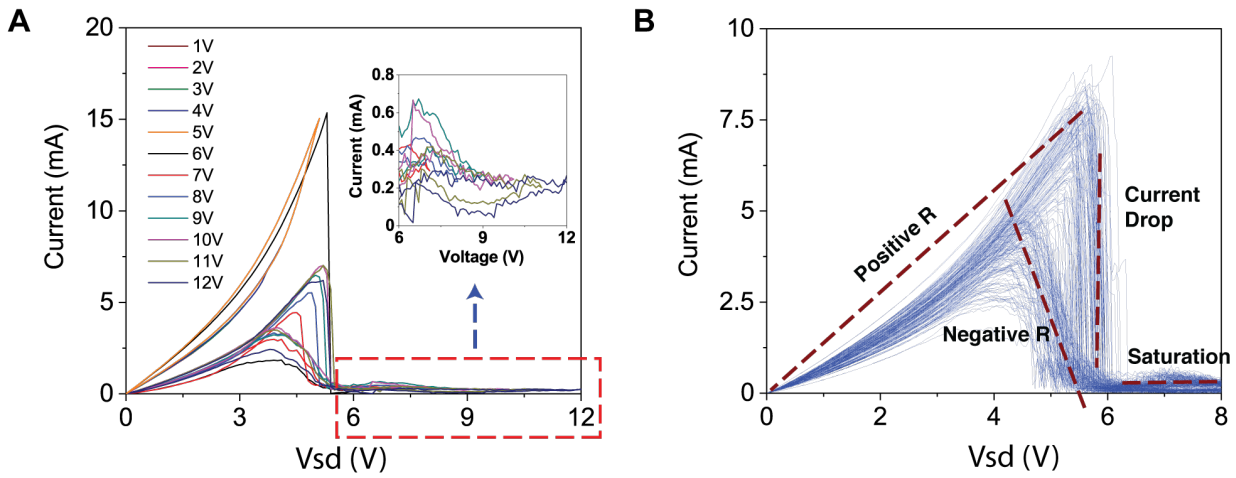

Fig. S11.

Multiple sweeps in W=7 µm and L=1 µm. A, IV characteristic was measured along with increasing bias voltage from 1 V to 12 V with forward and backward directions. **B**, 100 times multiple sweeps. Red dash lines show specific parameters, which are positive resistance (R), current drop, negative differential resistance (NDR), and saturation.

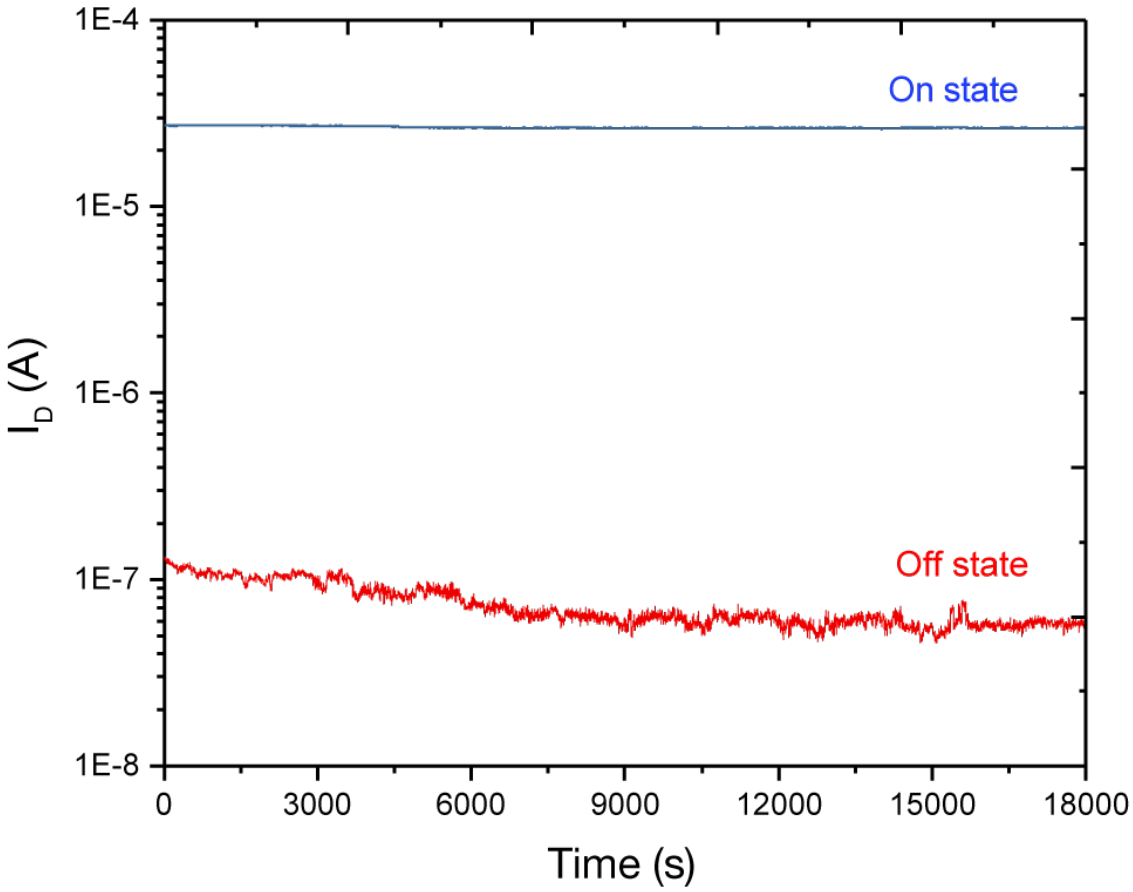

Fig. S12.
Drain current as a function of time in the "forward" and "reverse" states for 18,000 sec.

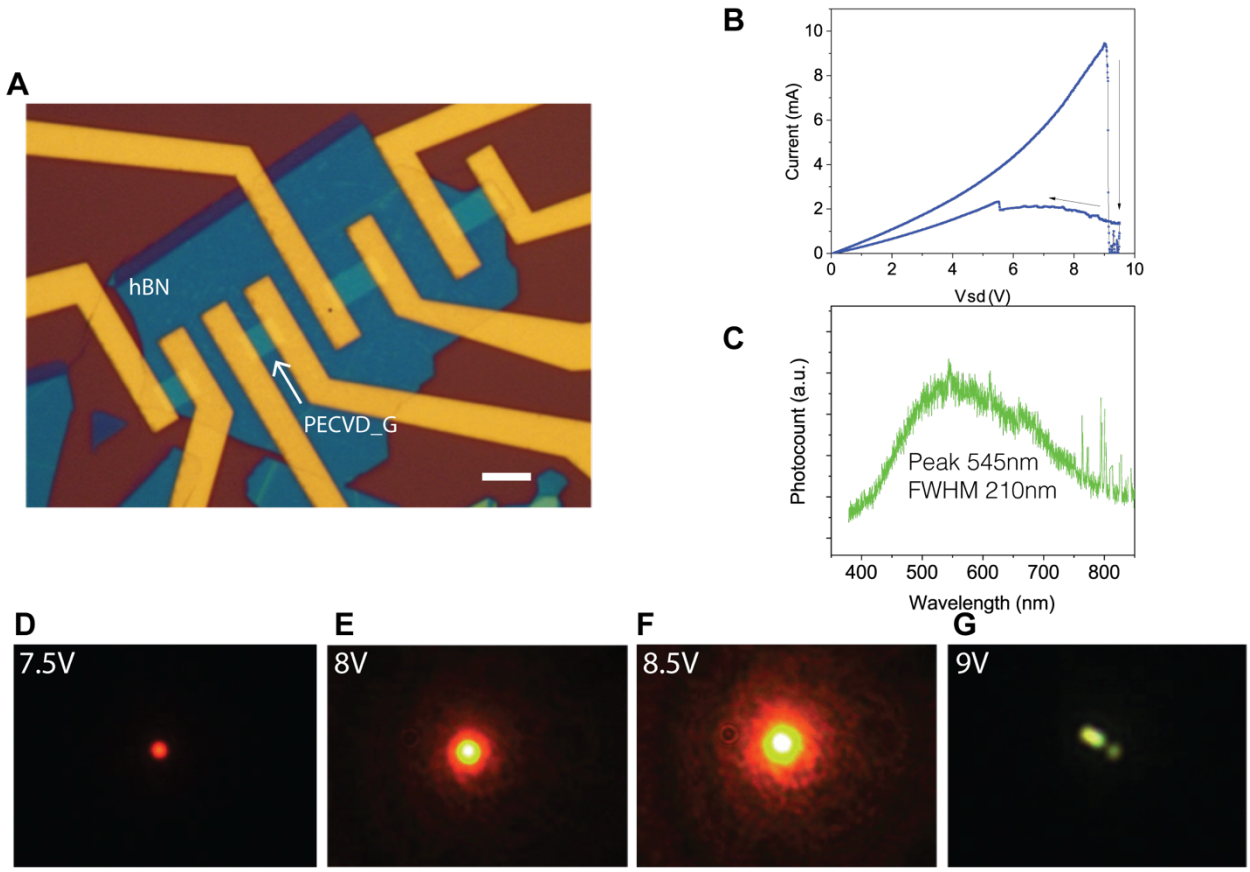

Fig. S13.

PECVD graphene on hBN. **A**, A microscope image of PECVD graphene on hBN having four channels. **B**, I-V characterization in which current abruptly drops in the forward sweep. **C**, EL spectroscopy. Peak wavelength is 545nm and FWHM is ~210nm. **D**, **E**, **F**, Each thermal radiation before current drop at 7.5V, 8V, 8.5V, respectively in a channel region with W=3 μm and L= 2 μm. **G**, Green light emission at 9V after the current drop.

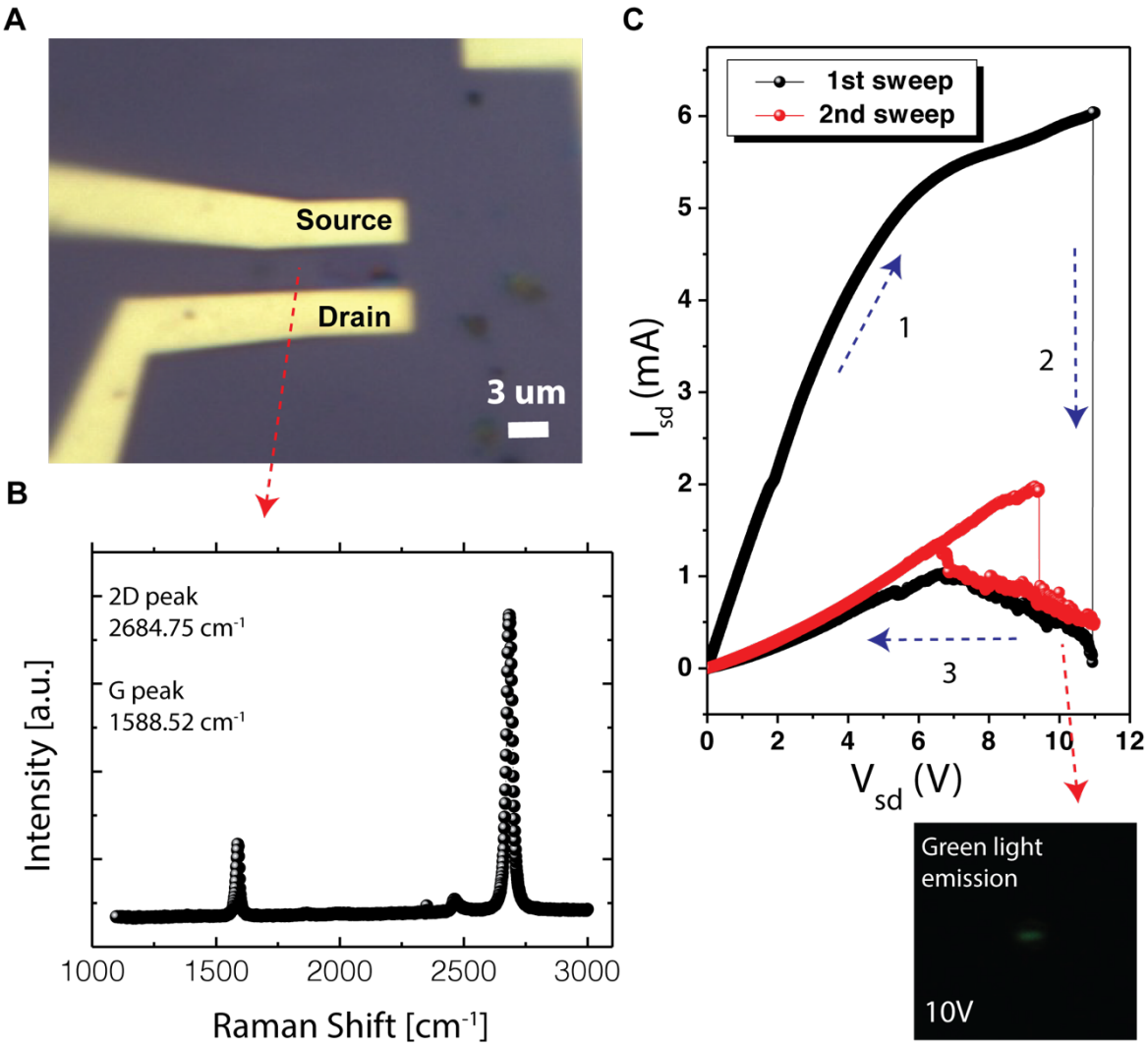

Fig. S14.

Exfoliated graphene light emitter (W=3 µm and L= 3 µm). A, A microscope image of exfoliated graphene on SiO_2 having 2 channels. **B**, Raman spectroscopy of exfoliated graphene. **C**, I-V characterization when current abruptly drops in sweep of forward and backward direction in first and second sweeps. Green light emission images at 10 V in the backward sweep has been shown here.

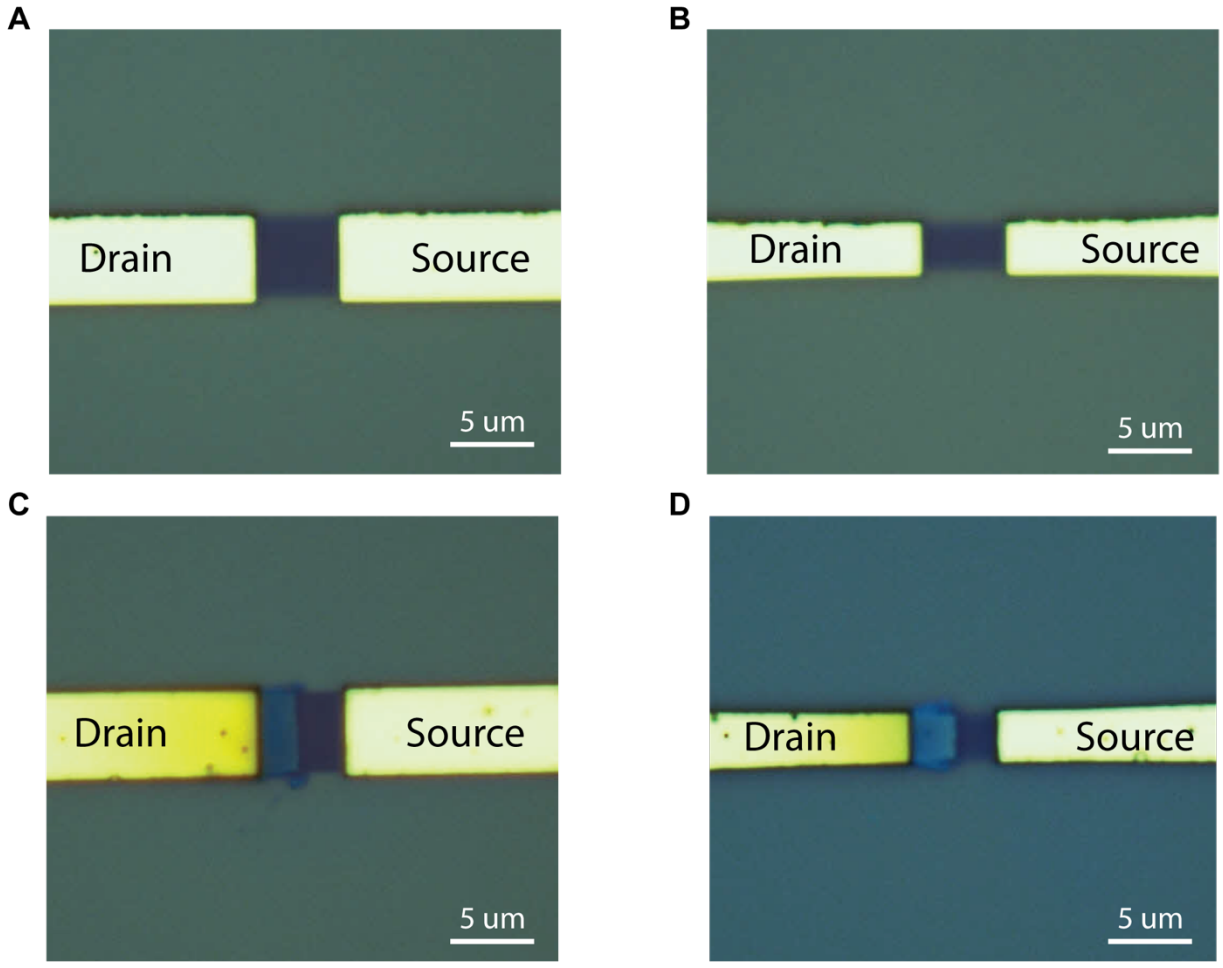

Fig. S15.

Microscope images before and after nanogap formation. PECVD graphene channels before (A, B) and after (C, D) nanogap formation. **A, C,** W=L=5 µm. **B, D,** W=3 µm, L=5 µm.

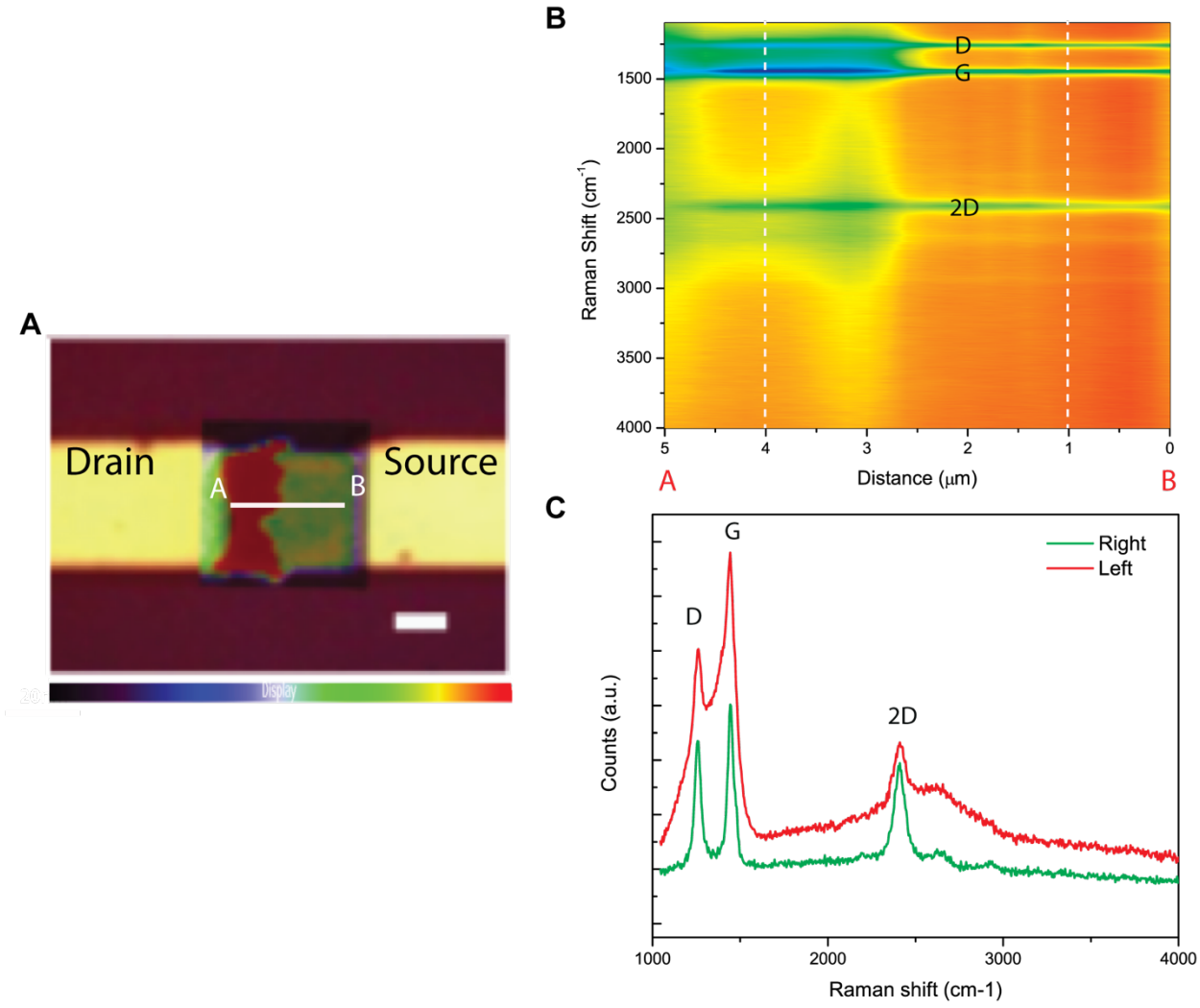

Fig. S16.

Raman mapping and representative data. A, G peak (1583 cm-1) Raman mapping of nanogap device (W=L=5 μm). Scale bar: 2.5 μm. **B**, 1D map of Raman shift in the cross line from A to B in (A). **C**, Raman shift at 4 μm (left) and 1 μm (right). Left side is showing graphene oxide having been merged with G (1583 cm^{-1}) and D (1350 cm^{-1}) peak.

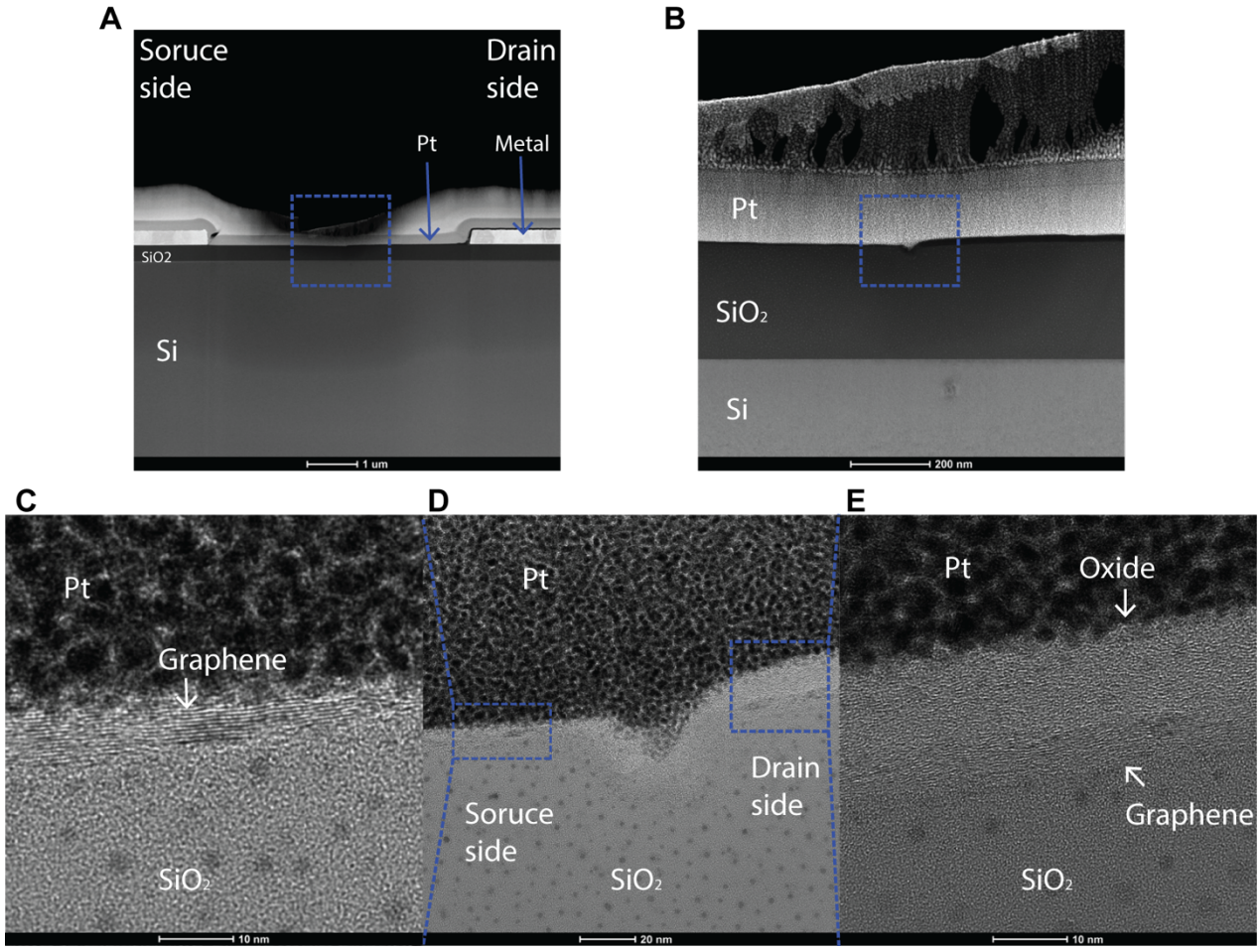

Fig. S17.

TEM measurement. A, HAADF image of the cross-section of the measured device. The Pt layer is deposited as a protective layer during the preparation of the cross-section, The approximately circular regions of dark regions are sample preparation artifacts and not part of the device structure, **B,** Enlarged image of the device revealing the graphene (5 nm), and graphene oxide (~20nm) layers. **C-E,** HRTEM images of the device where the graphene and graphene oxide meet at the junction (the scale of (C) and (E) is 10nm and one of (D) is 20nm).

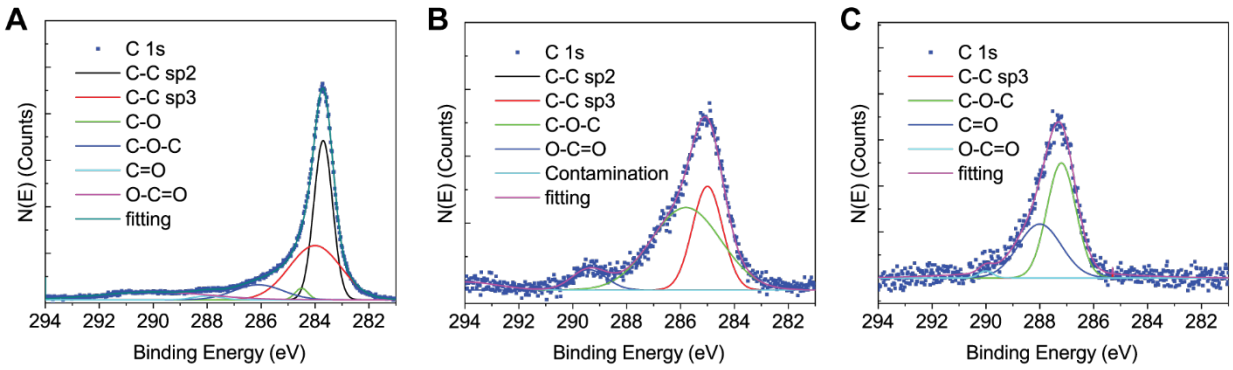

Fig. S18.

XPS measurement. The binding energy in C 1s of pristine PECVD graphene **(A),** graphene nanogap array **(B),** and oxidized PECVD graphene **(C)**.

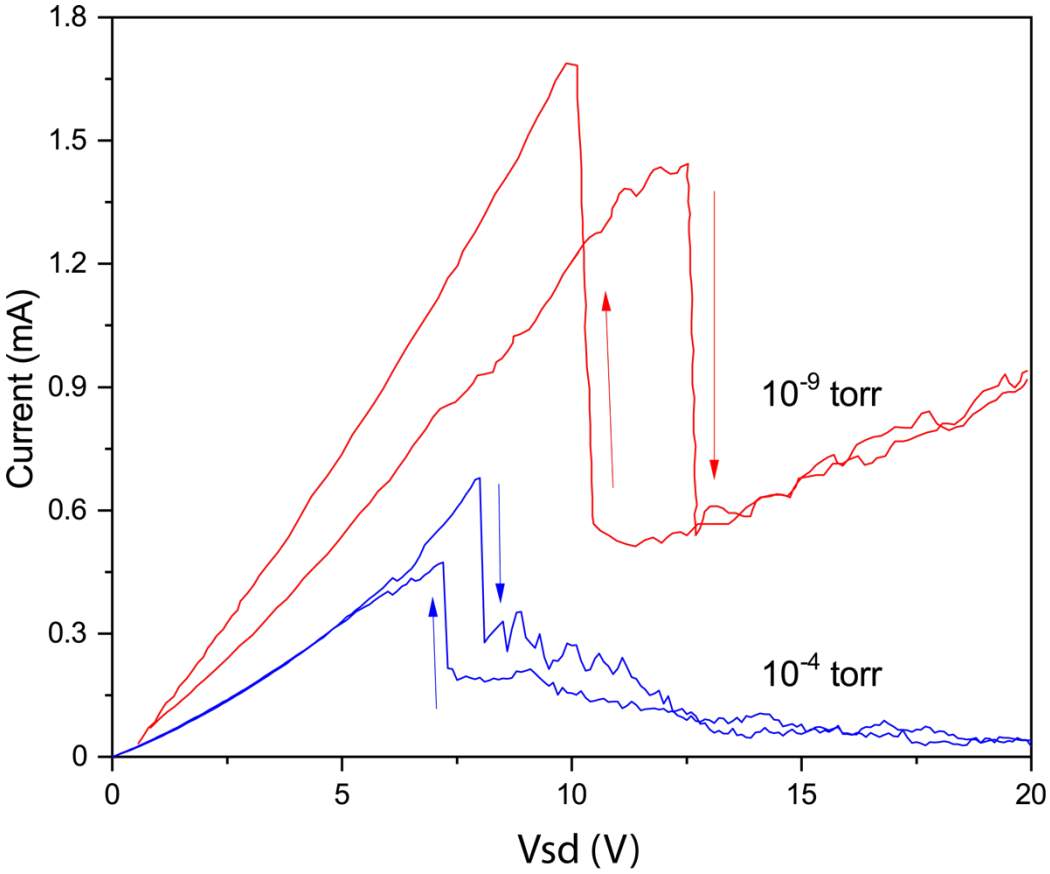

Fig. S19.

IV characterization in high and low vacuum. Red line was measured in 10^{-9} Torr and blue line in 10^{-4} Torr. The measured device size is W=L=5 μm.

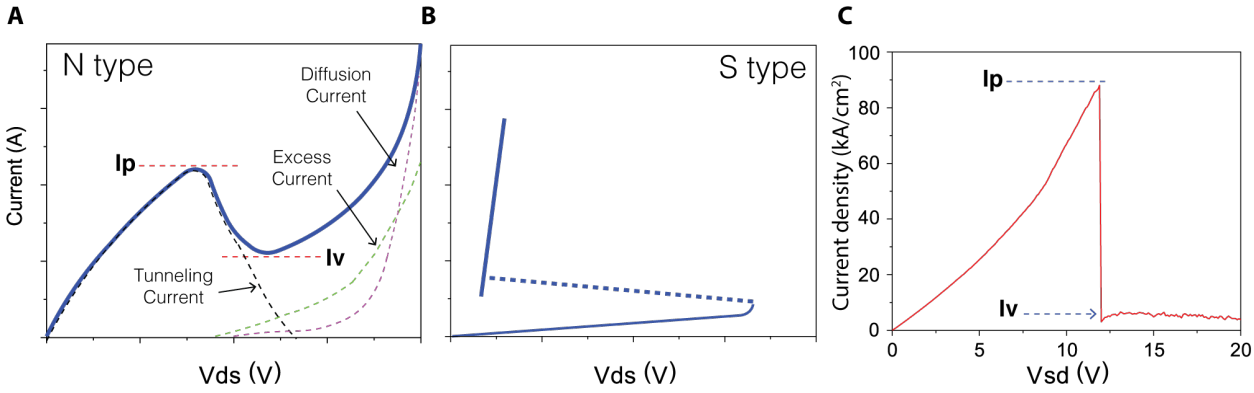

Fig. S20.

NDR types and unconventional behavior. A, N-type NDR. **B**, S-type NDR **C**, Unconventional IV characteristic of graphene nanogap device as current density (W=5 μm, L=5 μm).

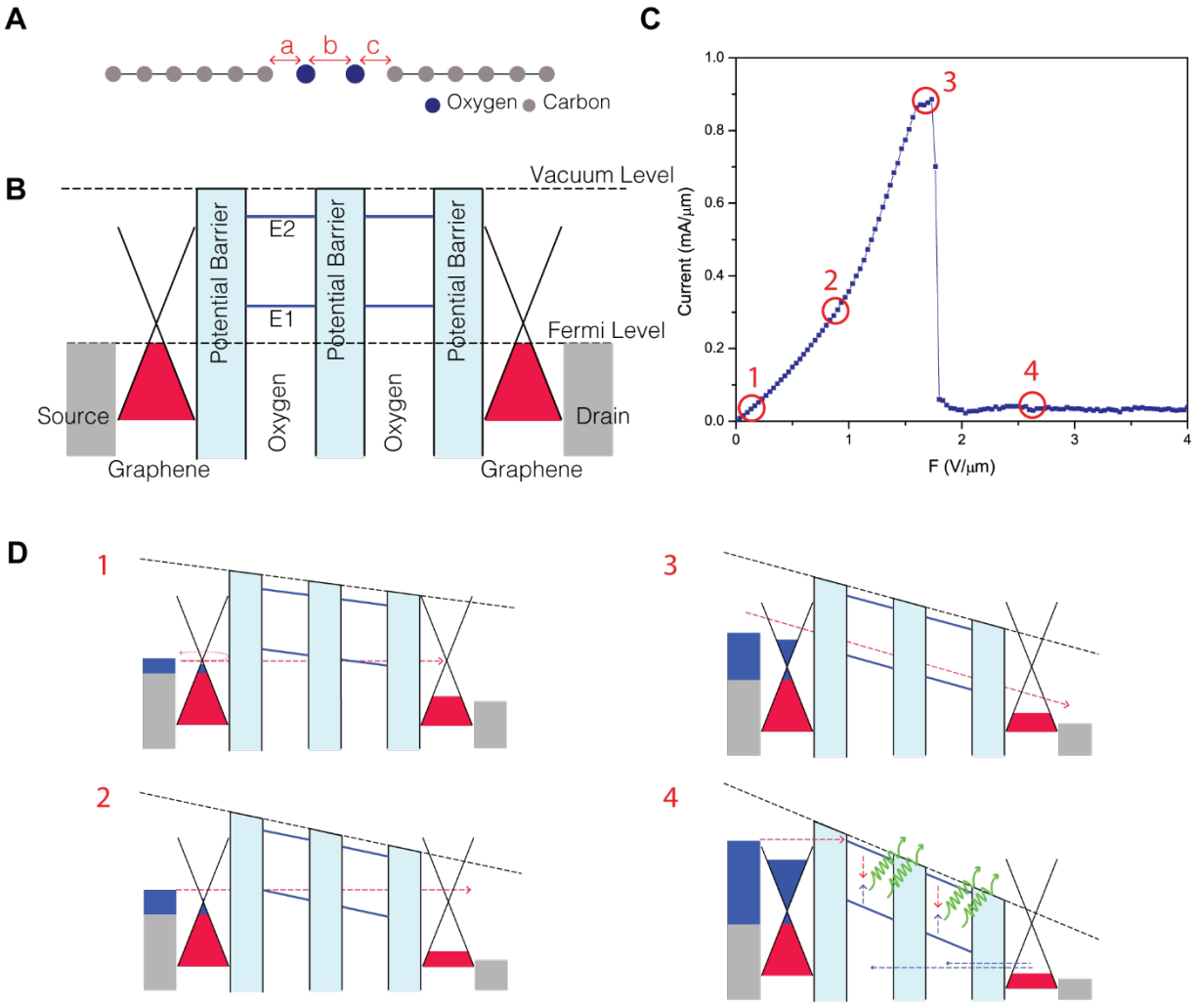

Fig. S21.

Nanogap modeling and multi quantum well structure. A, Atomic nanogap modeling in carbon chain including oxygen (for example, a=1.5 Å, b=2.5 Å, a=1.5 Å). **B**, Multi quantum well structure having metal contacts on highly p-doped graphene at zero bias. Quantum well width is assumed 1.5 Å which is the diameter of oxygen. The quantum well has ~2.3 eV of bandgap between two energy states. Each quantum well has two confined quantum states. **C**, Typical IV characterization of a graphene nanogap device. 1,2,3,4 circles are explained in D. **D**, **1**, Under E1 state, transmission rate is low and high reflection rate. **2**, On arriving at E1 state of Fermi level, the current increases fast with low resistance and high transmission rate. **3**, After passing E1 state of Fermi level, the current increases fast with low resistance and high transmission rate before current drop in C, **4**, Fermi level is close to the second energy states in the quantum well. Then holes in the drain can be allowed to pass the potential barriers and these holes can recombine with electrons in E2 state from the source. The excitons have ~2.3eV.

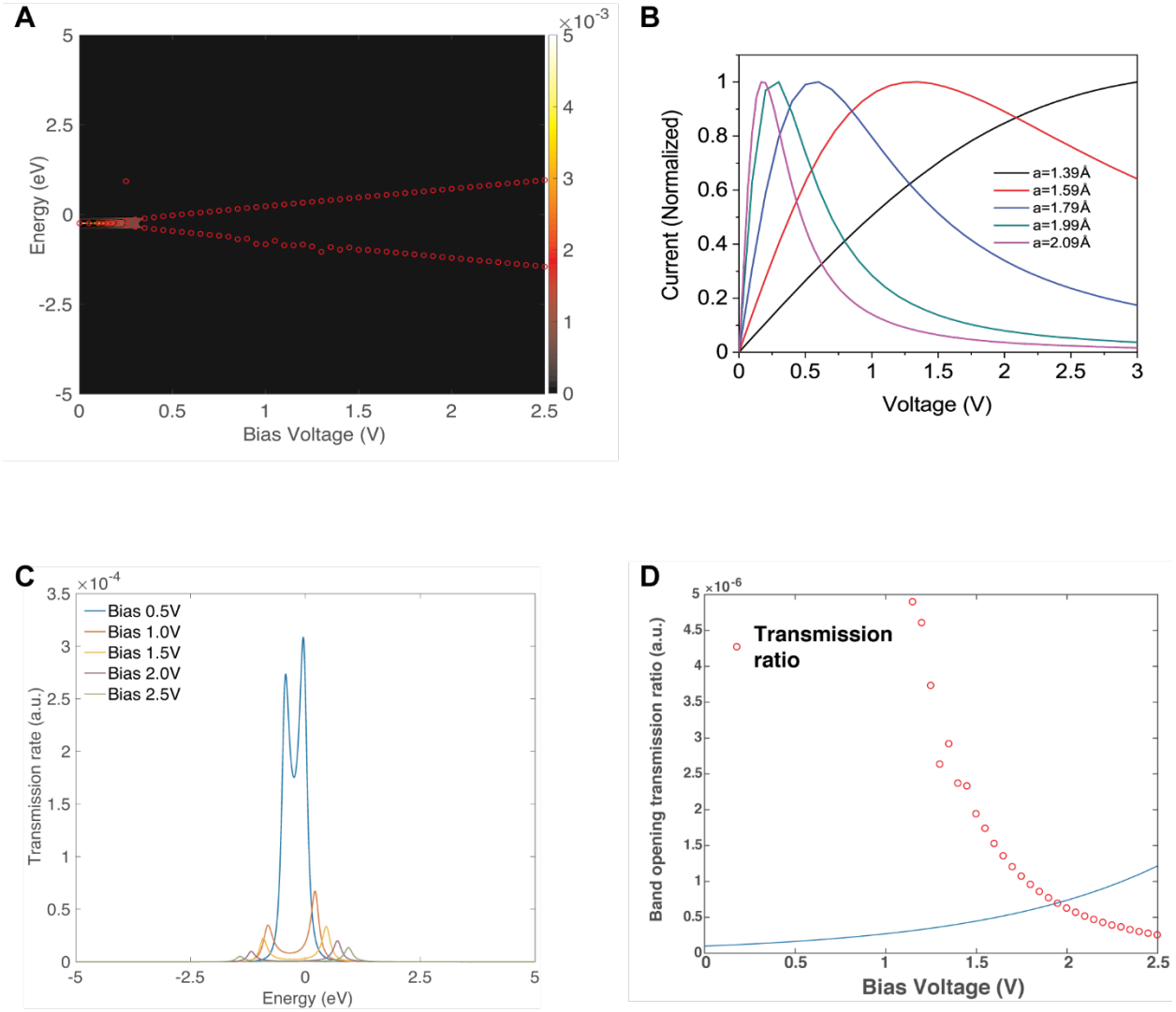

Fig. S22.

DFT calculation (C-C-C O O C-C-C). A, Transmission ratio mapping along with bias voltage. Red circles show peak transmission points. **B**, I-V characterization in the variation of distance parameters between C and O. **C**, From (a), transmission ratio at each 0.5 V bias step was depicted. **D**, Two-band separation occurs with increasing bias voltage. The blue line shows green light emission.

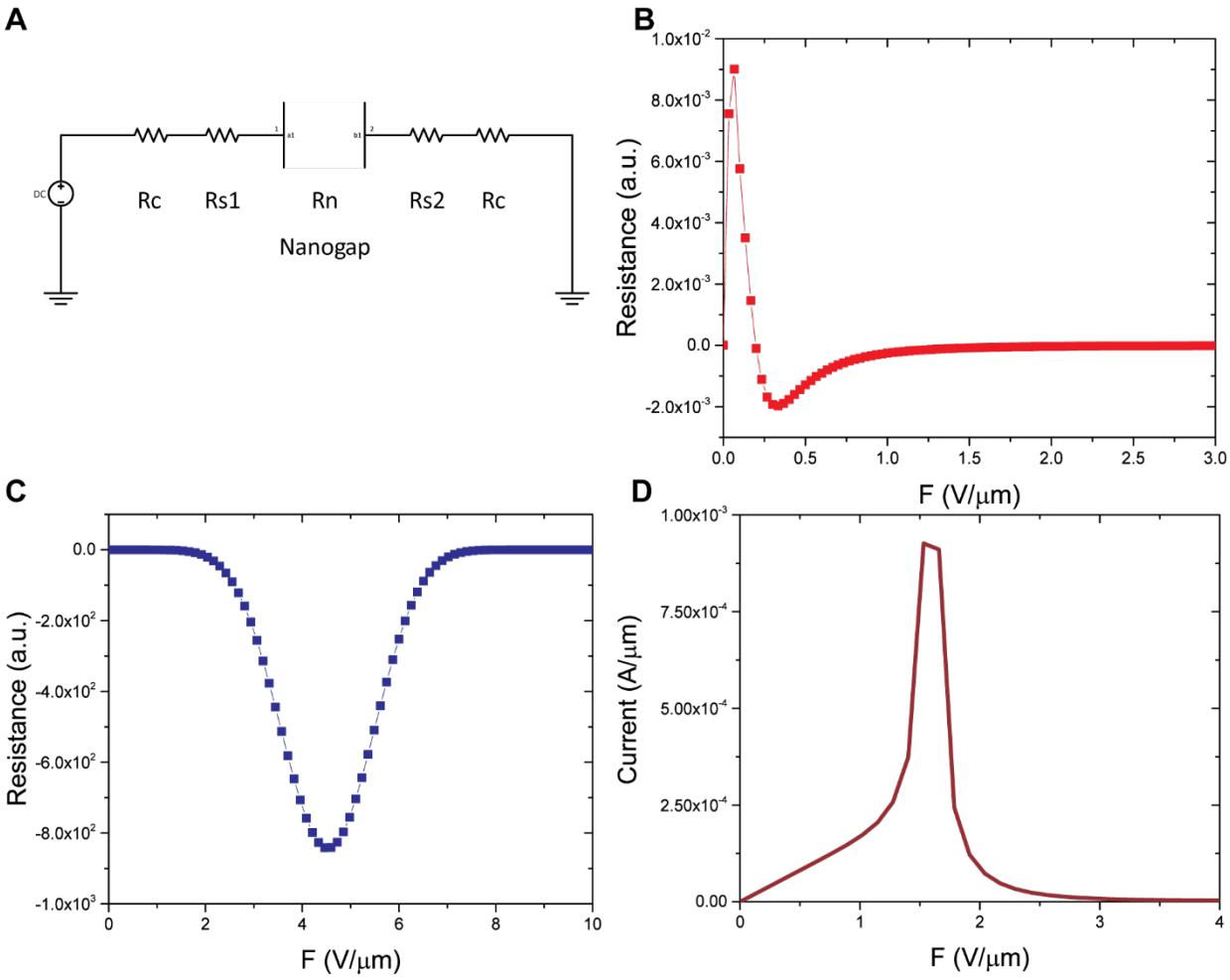

Fig. S23.

Circuit simulation. A, Circuit configuration. R_c is contact resistance. R_{s1} is graphene resistance. R_n is nanogap resistance extracted from DFT calculation. R_{s2} is graphene oxide resistance. **B**, R-V characterization in the nanogap device (Rn). **C**, From (A) and (B), total resistance variation can be simulated. **D**, I-V characterization based on (A), (B), and (C). Optimum scaling factors are reflected on the resistance of nanogap (R_n).

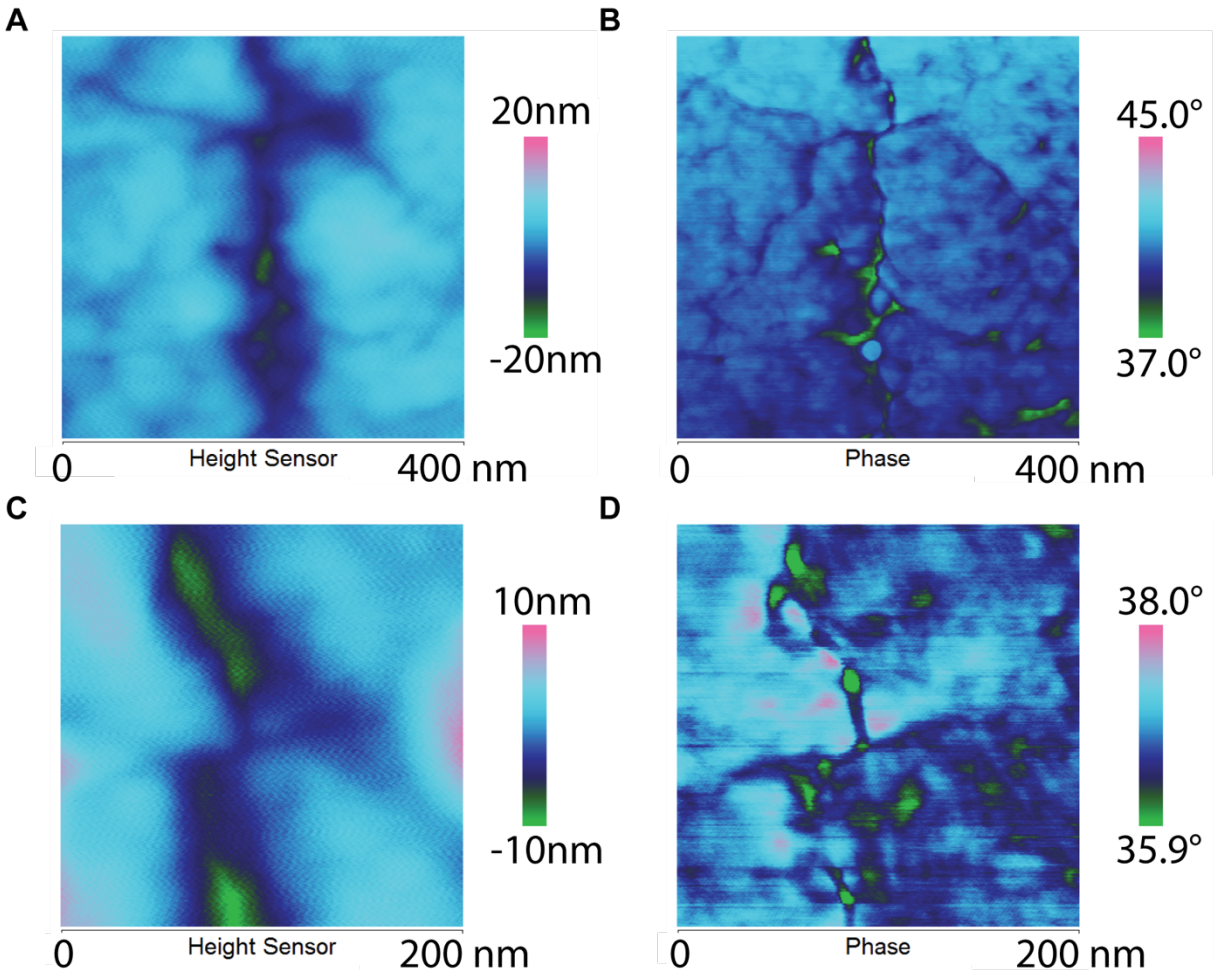

Fig. S24.

AFM images in nanogap. A, B, Height (A) and phase image (B) of nanogap region in the area of 400nm×400nm. **C, D,** Height (C) and phase image (D) of nanogap region in the area of 200nm×200nm.

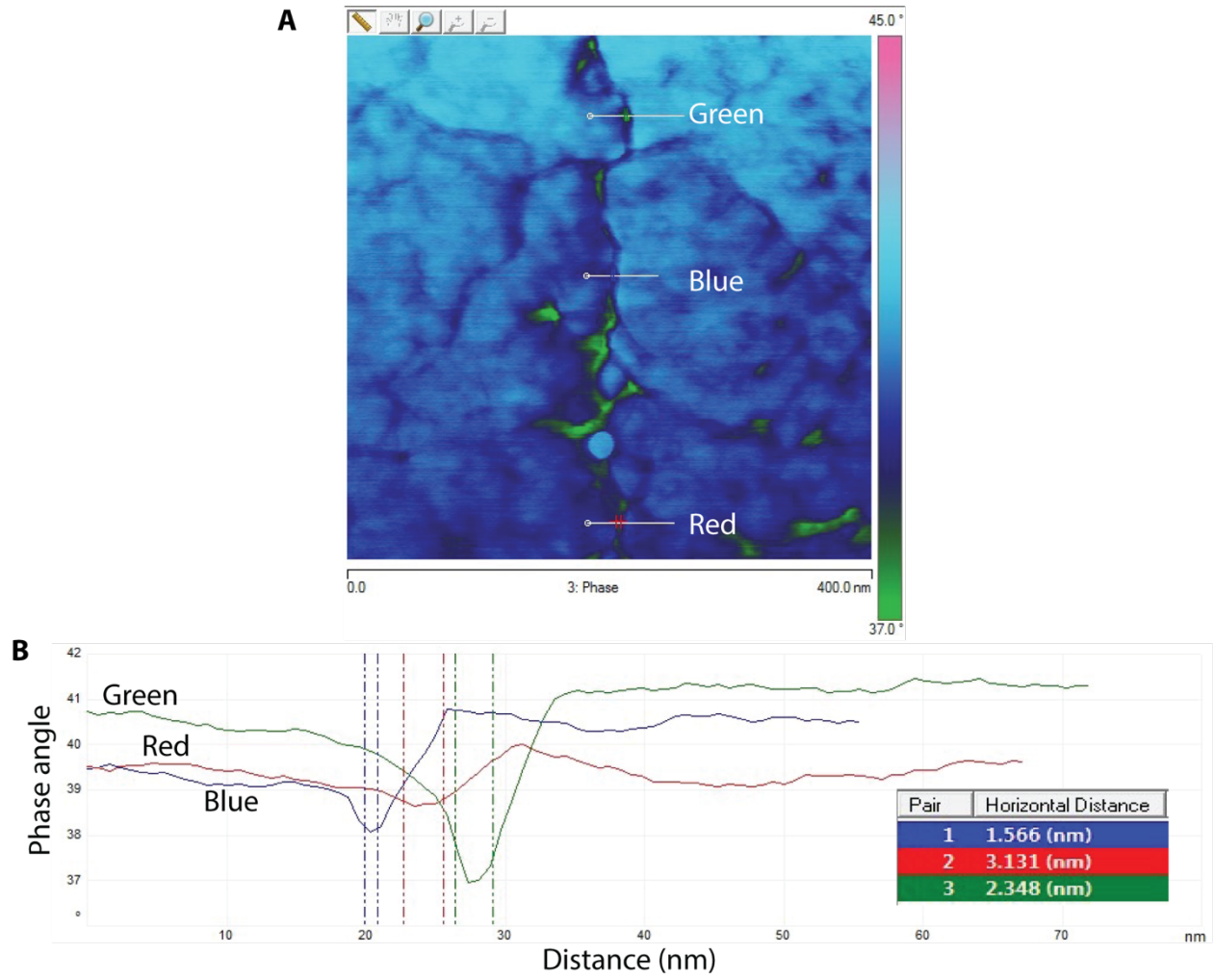

Fig. S25.

AFM line profiles in nanogap. A, Phase image of nanogap region in the area of 400nm×400nm. **B,** Line profiles in green, red, and blue cross lines on (A). Each two vertical line per color measures the horizontal distance as shown in the inset table, which is 1.566 nm (Blue), 3.131 nm (Red), 2.348 nm (Green), respectively.

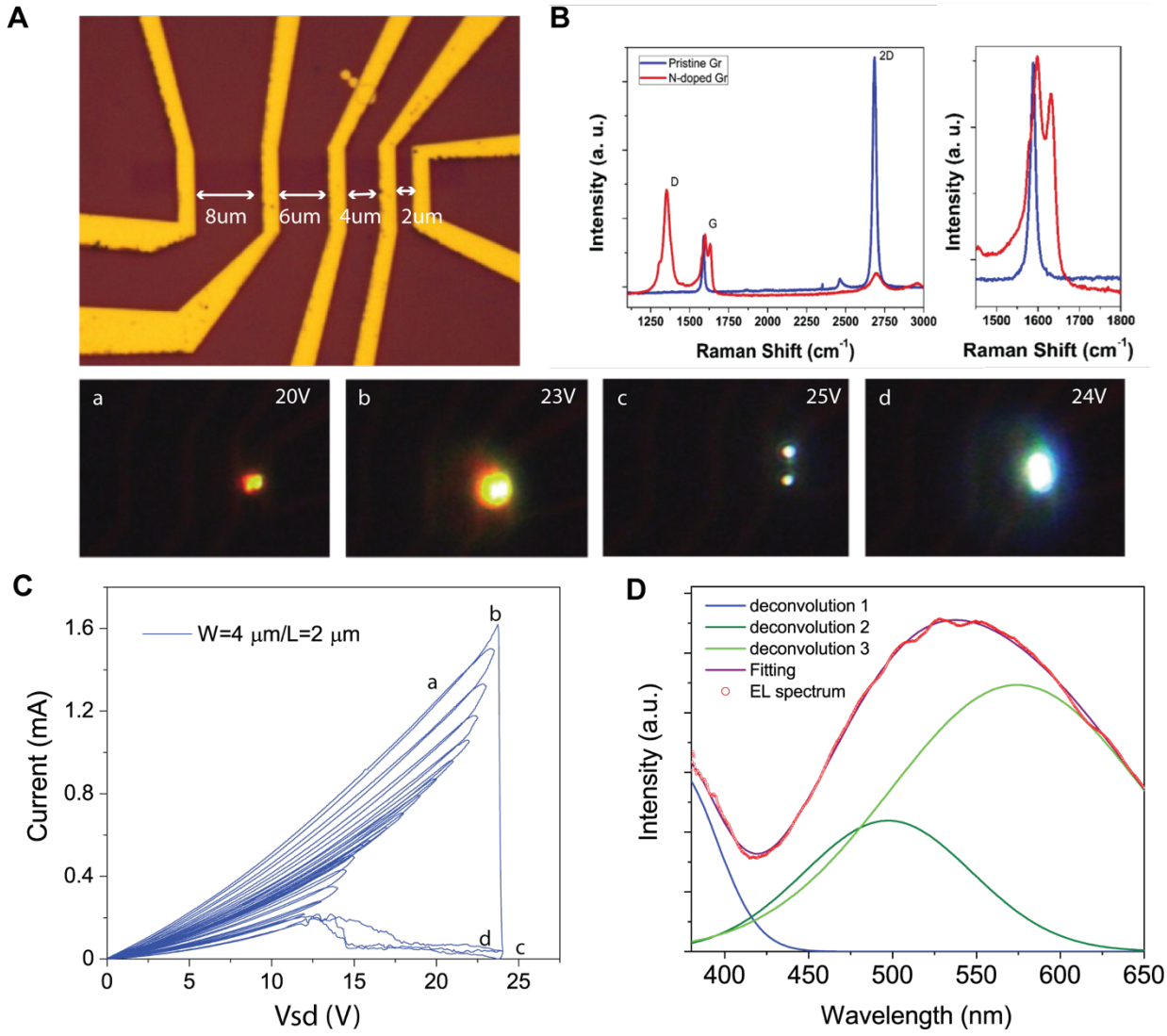

Fig. S26.

Nitrogen-doped graphene light emitter (W=4 μm and L= 2 μm). A, A microscope image of Nitrogen-doped graphene on SiO_2 having 4 channels. **B**, Raman spectroscopy of Nitrogen-doped graphene and intrinsic graphene. **C**, I-V characterization when current abruptly drops in sweep of forward and backward direction. Light emission images in a-d points on the graph are shown above (C). After breakdown, bluish light emission appears. **D**, EL spectroscopy. EL data was fitted and deconvoluted into three peaks. In blue emission, peak wavelength is 397 nm and FWHM is ~182 nm. In the other peaks, peak wavelengths are 497.3 nm and 574.2 nm, respectively.

Bonding	(a) PECVD graphene		(b) PECVD graphene nanogap array		(c) 1100°C oxygen annealing	
C-C sp^2	283.7 eV	39.20%	284 eV	~0 %	-	-
C-C sp^3	284 eV	36.70%	285 eV	31.70%	285.3 eV	~ 0 %
C-O	284.5 eV	1.95%	-	-	-	-
C-O-C	286.1 eV	9.69%	285.8 eV	58.42%	287.2 eV	49.85%
C=O	288 eV	1.39%	-	-	288 eV	48.69%
O-C=O	290 eV	11.02%	289.4 eV	7.19%	290 eV	1.45%
Contamination	-	-	294 eV	2.68%	-	-

Table S1.
De-convoluted XPS data of Fig. S18.

Supplementary Movie S1.
Nanogap formation in graphene channel which has W=5 μm, L=5 μm. Bias Voltage increases up to 16V by 0.2 V/sec.

Supplementary Movie S2.

Red and green light emission from nanogap graphene as measured with a microscope CCD camera. Bias voltages for this W=1 μm, L=1 μm graphene device was increased up to 12V by 0.2 V/sec.

Supplementary Movie S3.

A magnified version of Supplementary Movie S1.

Supplementary Movie S4.

16 × 4 arrays of nanogap graphene which has W=1 μm, L=1 μm.